International Association of Geodesy Symposia

Fernando Sansò, Series Editor

International Association of Geodesy Symposia

Fernando Sansò, Series Editor

Symposium 101: Global and Regional Geodynamics
Symposium 102: Global Positioning System: An Overview
Symposium 103: Gravity, Gradiometry, and Gravimetry
Symposium 104: Sea SurfaceTopography and the Geoid
Symposium 105: Earth Rotation and Coordinate Reference Frames
Symposium 106: Determination of the Geoid: Present and Future
Symposium 107: Kinematic Systems in Geodesy, Surveying, and Remote Sensing
Symposium 108: Application of Geodesy to Engineering
Symposium 109: Permanent Satellite Tracking Networks for Geodesy and Geodynamics
Symposium 110: From Mars to Greenland: Charting Gravity with Space and Airborne Instruments
Symposium 111: Recent Geodetic and Gravimetric Research in Latin America
Symposium 112: Geodesy and Physics of the Earth: Geodetic Contributions to Geodynamics
Symposium 113: Gravity and Geoid
Symposium 114: Geodetic Theory Today
Symposium 115: GPS Trends in Precise Terrestrial, Airborne, and Spaceborne Applications
Symposium 116: Global Gravity Field and Its Temporal Variations
Symposium 117: Gravity, Geoid and Marine Geodesy
Symposium 118: Advances in Positioning and Reference Frames
Symposium 119: Geodesy on the Move
Symposium 120: Towards an Integrated Global Geodetic Observation System (IGGOS)
Symposium 121: Geodesy Beyond 2000: The Challenges of the First Decade
Symposium 122: IV Hotine-Marussi Symposium on Mathematical Geodesy
Symposium 123: Gravity, Geoid and Geodynamics 2000
Symposium 124: Vertical Reference Systems
Symposium 125: Vistas for Geodesy in the New Millennium
Symposium 126: Satellite Altimetry for Geodesy, Geophysics and Oceanography
Symposium 127: V Hotine Marussi Symposium on Mathematical Geodesy
Symposium 128: A Window on the Future of Geodesy
Symposium 129: Gravity, Geoid and Space Missions
Symposium 130: Dynamic Planet - Monitoring and Understanding …
Symposium 131: Geodetic Deformation Monitoring: From Geophysical to Engineering Roles
Symposium 132: VI Hotine-Marussi Symposium on Theoretical and Computational Geodesy

VI Hotine-Marussi Symposium on Theoretical and Computational Geodesy

IAG Symposium
Wuhan, China
29 May - 2 June, 2006

Edited by

Peiliang Xu
Jingnan Liu
Athanasios Dermanis

Springer

Volume Editors

Dr. Peiliang Xu
Kyoto University
Disaster Prevention
Research Institute
Uji, Kyoto
611-0011
Japan

Professor Jingnan Liu
Wuhan University
GNSS Engineering Res. Center
430079 Wuhan
China

Professor Athanasios Dermanis
Aristotle University of Thessaloniki
Department of Geodesy & Surveying
University Box 503
54124 Thessaloniki
Greece

Series Editor

Professor Fernando Sansó
Polytechnic of Milan
D.I.I.A.R. – Surveying Section
Piazza Leonardo da Vinci, 32
20133 Milan
Italy

ISBN: 978-3-540-74583-9 e-ISBN: 978-3-540-74584-6

International Association of Geodesy Symposia ISSN: 0939-9585

Library of Congress Control Number: 2007933501

Cover Design: WMXDesign GmbH, Heidelberg

Printed on acid-free paper

9 8 7 6 5 4 3 2 1

springer.com

Preface

The famous Hotine-Marussi Symposium series is held once every four years and has been traditionally focused on mathematical geodesy. The VI Hotine-Marussi Symposium was organized by the Intercommission Committee on Theory (ICCT) and successfully held from 29 May to 2 June, 2006, at Wuhan University, PR China, with 162 registered scientists and students from 20 countries and regions, in addition to many more unregistered attendees. It was kindly sponsored by the International Association of Geodesy and Wuhan University.

The VI Hotine-Marussi Symposium was unique in the senses that: (i) this is the first Hotine-Marussi symposium to go beyond mathematical geodesy; (ii) this is the first time for a Hotine-Marussi symposium to be held outside Europe; and (iii) this is the first time that a Hotine-Marussi symposium was organized by an IAG entity instead of by Prof. F. Sanso and his group, as was traditionally the case. An attentive reader might soon notice the change of the title for the VI Hotine-Marussi Symposium. Indeed, this should be one of the most important aspects of the Symposium and was carefully designed as a result of many hours of discussion among Prof. A. Dermanis (ICCT Vice President), Prof. F. Sanso (IAG Past President and past organizer of the Hotine-Marussi symposia), Prof. J.N. Liu (President of Wuhan University) and P.L. Xu (ICCT President), in particular, also among the Scientific Committee members Prof. J.Y. Chen, Prof. B. Chao, Prof. H. Drewes, Prof. H.Z. Hsu, Prof. C. Jekeli, Dr. N.E. Neilan, Prof. C. Rizos and Prof. S.H. Ye.

In fact, as part of the IAG restructuring, the ICCT was formally approved and established after the IUGG XXIII Assembly in Sapporo, to succeed the former IAG Section IV on General Theory and Methodology, and more importantly, to actively and directly interact with other IAG Entities. The most important goals and/or targets of the ICCT are: (1) to strongly encourage frontier mathematical and physical research, directly motivated by geodetic need/practice, as a contribution to science/engineering in general and the foundations for Geodesy in particular; (2) to provide the channel of communication amongst the different IAG entities of commissions/services/projects, on the ground of theory and methodology, and directly cooperate with and support these entities in the topics-oriented work; (3) to help the IAG in articulating mathematical and physical challenges of geodesy as a subject of science and in attracting young talents to geodesy; and (4) to encourage closer research ties with and directly gets involved with relevant areas of the Earth Sciences, bearing in mind that geodesy has been playing an important role in understanding the physics of the Earth. In order to partly materialize the ICCT missions, we decided to use the VI Hotine-Marussi Symposium as a platform for promoting what we believe would be of most importance in the near future and for strengthening the interaction with commissions. This should clearly explain why we further decided to modify the traditional title of Hotine-Marussi symposia from "Mathematical Geodesy" to "Theoretical and Computational Geodesy", with a subtitle to emphasize challenge, opportunity and role of modern geodesy, and why you could see from our symposium programs that the IAG President Prof. G. Beutler, the IAG Secrectary General Prof. C.C. Tscherning and IAG commission Presidents Prof. H. Drewes, Prof. C. Rizos were invited to deliver invited talks at the Symposium, with our great honour, pleasure and gratitude.

Scientifically, recognizing that geodetic observing systems have advanced to such an extent that geodetic measurements:

(i) are now of unprecedented high accuracy and quality, can readily cover a region of any scale up to tens of thousands of kilometers, consist of non-conventional data types, and can be provided continuously;

(ii) consequently, demand new mathematical modeling in order to obtain best possible benefit of such technological advance; and
(iii) are finding applications that were either not possible due to accuracy limit or were not thought of as part of geodesy such as space weather and/or earth-environmental monitoring,

we designed and selected for the symposium the following five topics:

(i) Satellite gravity missions: open theoretical problems and their future application;
(ii) Earth-environmental, disaster monitoring and prevention by Geodetic methods;
(iii) GNSS: Mathematical theory, engineering applications, reference system definition and monitoring;
(iv) Deterministic and random fields analysis with application to Boundary Value Problems, approximation theory and inverse problems; and
(v) Statistical estimation and prediction theory, quality improvement and data fusion.

Some of these are either of urgent importance to geodesy or are of potentially fundamental importance to geodesy, but not necessarily limited to geodesy, at the very least, from our point of view. To name a few examples, let us say that: (i) satellite gravity missions are of current importance in and far beyond geodesy, environmental monitoring, for example; (ii) seafloor geodesy will become essential in the next one or two decades in Earth Sciences, even though the invited speakers could not find time to contribute their papers on the topic; and (iii) mixed integer linear models should be a subject that geodesists can make greatest possible contributions to mathematics and statistics.

Finally, we thank the International Association of Geodesy and Wuhan University for financial support. We thank all the conveners: B. Chao, D. Wolf, N. Sneeuw, J.T. Freymueller, K. Heki, C.K. Shum, Y. Fukuda, D.-N. Yuan, P. Teunissen, A. Dermanis, H. Drewes, Z. Altamimi, B. Heck, Karlsruhe, P. Holota, J. Kusche, B. Schaffrin, Y.Q. Chen, H. Kutterer and Y. Yang, for their hard work to convene and to take care of the review process of the Proceedings papers, which are essential to guarantee the success of the Symposium and the quality of the Proceedings. We also thank the LOC team, in particular, Dr. X. Zhang and Ms Y. Hu, for all their hard work.

Peiliang Xu
Jingnan Liu
Athanasios Dermanis

Contents

Part I: Satellite Gravity and Geodynamics

Part II: Reference Frame, GPS Theory, Algorithms and Applications

Part IV: Geodetic Boundary Value Problems and Inverse Problem Theory

Contributors

Z. Altamimi
Institut Géographique National, LAREG, 6-8 Avenue Blaise Pascal, 77455 Marne-la-Vallée, France

A.R. Amiri-Simkooei
Delft Institute of Earth Observation and Space Systems (DEOS), Delft University of Technology, Kluyverweg 1, 2629 HS Delft, The Netherlands, e-mail: a.amirisimkooei@TUDelft.nl

G. Austen
Stuttgart University, Geodetic Institute, Geschwister-Scholl-Str. 24/D, 70174 Stuttgart, Germany

J. Bao
Department of Hydrography and Cartography, Dalian Naval Academy, Dalian 116018, P.R. China

J. Bolte
GeoForschungsZentrum Potsdam, Telegrafenberg A17, 14473 Potsdam, Germany

C. Boucher
Conseil Général des Ponts et Chaussées, tour Pascal B, 92055 La Défense, France

J. Cai
Department of Geodesy and GeoInformatics, University of Stuttgart Geschwister-Scholl-Str. 24, D-70174 Stuttgart, Germany, e-mail: cai@gis.uni-stuttgart.de

Z. Cai
Global Information Application and Development Center of Beijing, 100094 Beijing, P.R. China

B. Chao
The School of Geodesy and Geomatics, Wuhan University, Wuhan, P.R. China

B.F. Chao
College of Earth Sciences, National Central University, Taiwan; also NASA Goddard Space Flight Center, USA

D.B. Chao
The Key Laboratory of Geospace Environment and Geodesy, Ministry of Education, School of Geodesy and Geomatics, Wuhan University, Wuhan 129 Luoyu Road, Wuhan 430079, P.R. China

J. Chen
Department of Surveying and Geo-informatics, Tongji University, Siping Road 1239, 200092 Shanghai, P.R. China; GeoForschungsZentrum Potsdam, Telegrafenberg A17, 14473 Potsdam, Germany

Y. Chen
Geodetic Science, School of Earth Sciences, The Ohio State University, 125 S. Oval Mall, 275 Mendenhall Lab., Columbus, Ohio 43210, USA, e-mail: chen.862@osu.edu

X. Collilieux
Institut Géographique National, LAREG, 6–8 Avenue Blaise Pascal, 77455 Marne-la-Vallée, France

S. Cravoisier
Laboratoire de Géodynamique des Rifts et des Marges Passives (LGRMP), Université du Maine, UFR Sciences et Techniques, Bât. Géologie, Avenue O. Messiaen, F-72085 Le Mans Cedex 09, France

W.J. Dai
Department of Survey Engineering and Geomatics, Central South University, Changsha, Hunan Province 410083, P.R. China

A. Dermanis
Department of Geodesy and Surveying, Aristotle University of Thessaloniki, University Box 503, 54124 Thessaloniki, Greece

X. Ding
Department of Land Surveying and Geo-Informatics, The Hong Kong Polytechnic University, Hung Hom, Kowloon, Hong Kong, P.R. China

P. Ditmar
Delft Institute of Earth Observation and Space Systems (DEOS), Delft University of Technology, Kluyverweg 1, P.O. Box 5058, 2600 GB Delft, The Netherlands

C. Dorbath
Institut Physique du Globe de Strasbourg (IPGS), 5 Rue René Descartes, F-67084 Strasbourg Cedex, France

S. Durand
Laboratoire de Géodésie et Géomatique (L2G), Ecole Supérieure des Géomètres et Topographes (ESGT/CNAM), 1 Boulevard Pythagore, F-72000 Le Mans, France

M. El-Habiby
Department of Geomatics Engineering, The University of Calgary, 2500 University Drive N.W., Calgary, Alberta, Canada T2N 1N4

P. Fan
Zhengzhou Institute of Surveying and Mapping, 66th Longhai Middle Road, Zhengzhou 450052, P.R. China

Y.A. Felus
Surveying Engineering Department, Ferris State University, Big Rapids, Michigan, USA

R. Forsberg
Geodynamic department, Danish National Space Center, Juliane Maries Vej 30, 2100 Copenhagen, Denmark

W. Freeden
University of Kaiserslautern, Geomathematics Group, 67653 Kaiserslautern, P.O. Box 3049, Germany, e-mail: freeden@mathematik.uni-kl.de

B. Gao
Civil Engineering Department, Shijiazhuang Railway Institute, Shijiazhuang 050043, P.R. China

M.R. Ge
GNSS Research Center, Wuhan University, Wuhan, Hubei, P.R. China

J.H. Geng
GNSS Research Center, Wuhan University, Wuhan, Hubei, P.R. China

L. Geoffroy
Laboratoire de Géodynamique des Rifts et des Marges Passives (LGRMP), Université du Maine, UFR Sciences et Techniques, Bât. Géologie, Avenue O. Messiaen, F-72085 Le Mans Cedex 09, France

E.W. Grafarend
Department of Geodesy and GeoInformatics, University of Stuttgart Geschwister-Scholl-Str. 24, D-70174 Stuttgart, Germany

S. Gramsch
University of Kaiserslautern, Geomathematics Group, 67653 Kaiserslautern, P.O. Box 3049, Germany, e-mail: gramsch@mathematik.uni-kl.de

V. Grund
GeoForschungsZentrum Potsdam, Telegrafenberg A17, 14473 Potsdam, Germany

Q. Gui
Institute of Science, Information Engineering University, No. 62, Kexue Road, Zhengzhou 450001, Henan, P.R. China

B. Gundlich
Central Institute for Electronics Forschungszentrum Jülich GmbH, 52425 Jülich, Germany; GFZ Potsdam, Telegrafenberg, 14473 Postdam, Germany

J. Guo
The School of Geodesy and Geomatics, Wuhan University, Wuhan, P.R. China

B. Han
School of Architectural Engineering, Shandong University of Technology, Zibo, P.R. China

S. Han
Institute of Science, Information Engineering University, No. 62, Kexue Road, Zhengzhou 450001, Henan, P.R. China

B. Heck
Geodetic Institute, University of Karlsruhe, Englerstr 7, D-76128 Karlsruhe, Germany

P. Holota
Research Institute of Geodesy, Topography and Cartography, 25066 Zdiby 98, Praha-východ, Czech Republic, e-mail: holota@pecny.asu.cas.cz

C. Hu
Department of Surveying and Geo-informatics, Tongji University, Siping Road 1239, 200092 Shanghai, P.R. China

D. Huang
Department of Geomatic Engineering, Southwest Jiaotong University, Chendu 610031, P.R. China

J. Huang
School of Geodesy and Geomatics, Wuhan University, Wuhan, China

K.H. Ilk
Institute of Theoretical Geodesy, University of Bonn, Nussallee 17, D-53115 Bonn, Germany

W.P. Jiang
School of Geodesy and Geomatics, Wuhan University, 129 Luoyu Road, Wuhan 430079, P.R. China

W. Keller
Stuttgart University, Geodetic Institute, Geschwister-Scholl-Str. 24/D, 70174 Stuttgart, Germany

J. Klotz
GeoForschungsZentrum Potsdam, Telegrafenberg A17, 14473 Potsdam, Germany

H. Koivula
Department of Geodesy and Geodynamics, Finnish Geodetic Institute, Geodeetinrinne 2, FI-02430 Masala, Finland

C. Kotsakis
Department of Geodesy and Surveying, Aristotle University of Thessaloniki, University Box 440, GR-54124, Thessaloniki, Greece, e-mail: kotsaki@topo.auth.gr

M.N. Kulkarni
Department of Civil Engineering, Indian Institute of Technology Bombay, Powai, Mumbai 400076, India, e-mail: kulkarni@iitb.ac.in

J. Kusche
Delft Institute of Earth Observation and Space Systems (DEOS), TU Delft, Kluyverweg 1, P.O. Box 5058, 2600 GB Delft, The Netherlands; GFZ Potsdam, Telegrafenberg, 14473 Potsdam, Germany

H. Kutterer
Geodetic Institute, Leibniz University of Hannover, Nienburger Straße 1, D-30167 Hannover, Germany

A.Q. Le
Delft Institute of Earth Observation and Space Systems (DEOS), Delft University of Technology, Delft, The Netherlands

B. Li
Department of Surveying and Geo-informatics, Tongji University, 1239 Siping Road, Shanghai 200092, P.R. China

C. Li
Center for Geomation Engineering, Southwest Jiaotong University, Chengdu, P.R. China

J.C. Li
The Key Laboratory of Geospace Environment and Geodesy, Ministry of Education, School of Geodesy and Geomatics, Wuhan University, 129 Luoyu Road, Wuhan 430079, P.R. China

M. Li
Department of Hydrography and Cartography, Dalian Naval Academy, Dalian 116018, P.R. China; Geomatics and Applications Laboratory, Liaoning Technical University, Fuxin 123000, P.R. China; Institute of Surveying and Mapping, Information Engineering University, Zhenzhou 450052, P.R. China

S. Li
Civil Engineering Department, Shijiazhuang Railway Institute, Shijiazhuang 050043, P.R. China; College of Geodesy and Geomatics, Wuhan University, Wuhan 430079, P.R. China

W. Li
Civil Engineering Department, Shijiazhuang Railway Institute, Shijiazhuang 050043, P.R. China

Z. Li
Department of Land Surveying and Geo-Informatics, The Hong Kong Polytechnic University, Hung Hom, Kowloon, Hong Kong, P.R. China

Z.W. Li
Department of Survey Engineering and Geomatics, Central South University, Changsha, Hunan Province 410083, P.R. China

C. Liu
School of Geodesy and Geomatics, Wuhan University, Wuhan, China

J. Liu
School of Geodesy and Geomatics, Wuhan University, 129, Luoyu Road, Wuhan, China

J.N. Liu
GNSS Research Center, Wuhan University, Wuhan, Hubei, P.R. China

X. Liu
Delft Institute of Earth Observation and Space Systems (DEOS), Delft University of Technology, Kluyverweg 1, P.O. Box 5058, 2600 GB Delft, The Netherlands, e-mail: x.l.liu@tudelft.nl

Y.C. Liu
Department of Hydrography and Cartography, Dalian Naval Academy, Dalian 116018, P.R. China; Geomatics and Applications Laboratory, Liaoning Technical University, Fuxin 123000, P.R. China; Institute of Surveying and Mapping, Information Engineering University, Zhenzhou 450052, P.R. China

Y.Y. Liu
Zhengzhou Institute of Surveying and Mapping, 66th Longhai Middle Road, Zhengzhou 450052, P.R. China

A. Löcher
Institute of Theoretical Geodesy, University of Bonn, Nussallee 17, D-53115 Bonn, Germany

N. Luo
The School of Geodesy and Geomatics, Wuhan University, Wuhan, P.R. China

Z. Lv
Institute of Surveying and Mapping, Information Engineering University, Zhenzhou 450052, P.R. China

C. Ma
Institute of Science, Information Engineering University, No. 62, Kexue Road, Zhengzhou, 450001 Henan, P.R. China

T. Mayer-Gürr
Institute of Theoretical Geodesy, University of Bonn, Nussallee 17, D-53115 Bonn, Germany

J.F.G. Monico
Department of Cartography, São Paulo State University, UNESP, Roberto Simonsen, 305, Pres. Prudente, SP, Brazil

M. Moreno
GeoForschungsZentrum Potsdam, Telegrafenberg A17, 14473 Potsdam, Germany

O. Nesvadba
Land Survey Office, Pod Sídlištěm 9, 182 11 Praha 8, Czech Republic, e-mail: nesvadba@bonbox.cz

I. Neumann
Geodetic Institute, Leibniz University of Hannover, Nienburger Straße 1, D-30167 Hannover, Germany

J. Nicolas
Laboratoire de Géodésie et Géomatique (L2G), Ecole Supérieure des Géomètres et Topographes (ESGT/CNAM), 1 Boulevard Pythagore, F-72000 Le Mans, France

D. Odijk
Delft Institute of Earth Observation and Space Systems (DEOS), Delft University of Technology, Kluyverweg 1, 2629 HS Delft, The Netherlands, e-mail: d.odijk@TUDelft.nl

A. Pagamisse
Department of Mathematics, São Paulo State University, UNESP, Roberto Simonsen, 305, Pres., Prudente, SP, Brazil

T. Peters
Institute of Astronomical and Physical Geodesy, Technische Universität München, Arcisstr. 21, D-80290 München, Germany, e-mail: peters@bv.tum.de

D. Petrovich
Institute of Mathematics, Tampere University of Technology, P.O. Box 553, 33101 Tampere, Finland

R. Piché
Institute of Mathematics, Tampere University of Technology, P.O. Box 553, 33101 Tampere, Finland

W.G.C. Polezel
Department of Cartography, São Paulo State University, UNESP, Roberto Simonsen, 305, Pres., Prudente, SP, Brazil

M. Poutanenr
Department of Geodesy and Geodynamics, Finnish Geodetic Institute, Geodeetinrinne 2, FI-02430 Masala, Finland

M. Reguzzoni
Italian National Institute of Oceanography and Applied Geophysics (OGS), c/o Politecnico di Milano, Polo Regionale di Como, Via Valleggio, 11, 22100 Como, Italy

C. Rizos
School of Surveying and Spatial Information Systems, University of New South Wales, Sydney, NSW 2052, Australia

M. Roggero
Politecnico di Torino, Department of Land Engineering, Environment and Geotechnologies, Corso Duca degli Abruzzi 24, 10129, Torino, Italy, e-mail: roggero@atlantic.polito.it

D.R. Roman
National Geodetic Survey, Silver Spring, MD 20910, USA

F. Sacerdote
Dipartimento di Ingegneria Civile, Università di Firenze, Via S. Marta 3, 50139 Firenze, Italy

J. Saleh
National Geodetic Survey, Silver Spring, MD 20910, USA

L. Sánchez
Deutsches Geodätisches Forschungsinstitut, DGFI, Alfons-Goppel-Str. 11, D-80539 Munich, Germany

F. Sansò
DIIAR, Politecnico di Milano, Polo Regionale di Como, Via Valleggio, 22100 Como, Italy

B. Schaffrin
Geodetic Science Program, School of Earth Sciences, The Ohio State University, 125 S. Oval Mall, 275 Mendenhall Lab., Columbus, Ohio 43210, USA

M. Schreiner
University of Buchs, Laboratory for Industrial Mathematics, Werdenbergstrasse 4, CH-9471 Buchs, Switzerland, e-mail: schreiner@ntb.ch

M.A. Sharifi
Institute of Geodesy, Universität Stuttgart, Geschwister-Scholl-Str. 24D, D-70174 Stuttgart, Germany

C. Shen
Institute of Seismology, CEA, Wuhan 430071, P.R. China

Y. Shen
Department of Surveying and Geo-informatics, Tongji University, 1239 Siping Road, Shanghai 200092, P.R. China

C. Shi
GNSS Research Center, Wuhan University, Wuhan, Hubei, P.R. China

C.K. Shum
Geodetic Science, School of Earth Sciences, The Ohio State University, 125 S. Oval Mall, 275 Mendenhall Lab., Columbus, Ohio 43210, USA

M.G. Sideris
Department of Geomatics Engineering, University of Calgary, 2500 University Drive N.W., Calgary, Alberta, Canada T2N 1N4, e-mail: sideris@ucalgary.ca

N. Sneeuw
Geodätisches Institut, Stuttgart Universität, Stuttgart D-70147, Germany, e-mail: sneeuw@gis.uni-stuttgart.de

E.M. Souza
Department of Cartography, São Paulo State University, UNESP, Roberto Simonsen, 305, Pres., Prudente, SP, Brazil

L. Sui
Zhengzhou Institute of Surveying and Mapping, 66th Longhai Middle Road, Zhengzhou 450052, P.R. China, e-mail: suilifen@163.com

S. Sun
Institute of Seismology, CEA, Wuhan 430071, P.R. China

P.J.G. Teunissen
Delft Institute of Earth Observation and Space systems (DEOS), Delft University of Technology, Kluyverweg 1, 2629 HS Delft, The Netherlands, e-mail: P.J.G.Teunissen@TUDelft.nl

H. Tian
School of Geodesy and Geomatics, Wuhan University, Wuhan, China

C.C.J.M. Tiberius
Delft institute of Earth Observation and Space systems (DEOS), Delft University of Technology, Kluyverweg 1, 2629 HS Delft, The Netherlands

N. Tselfes
DIIAR, Politecnico di Milano, Polo Regionale di Como, Via Valleggio, 11, 22100 Como, Italy

J.P. van Loon
Delft Institute of Earth Observation and Space Systems (DEOS), TU Delft, Kluyverweg 1, P.O. Box 5058, 2600 GB Delft, The Netherlands

G. Venuti
DIIAR, Politecnico di Milano, Polo Regionale di Como, Via Valleggio, 11, 22100 Como, Italy

S. Verhagen
Delft Institute of Earth Observation and Space systems, Delft University of Technology, Kluyverweg 1, 2629 HS Delft, The Netherlands, e-mail: a.a.verhagen@TUDelft.nl

J. Wang
Department of Surveying and Geo-informatics, Tongji University, Siping Road 1239, 200092 Shanghai, P.R. China

W. Wang
The School of Geodesy and Geomatics, Wuhan University, P.R. China, e-mail: wangwei_sgg@163.com

W. Wang
Zhengzhou Institute of Surveying and Mapping, 66th Longhai Middle Road, Zhengzhou 450052, P.R. China

X. Wang
School of Geodesy & Geomatics, Wuhan University, 129 Luoyu Road, Wuhan 430079, P.R. China; Key Laboratory of Geomatics and Digital Technology of Shandong Province, Shandong University of Science and Technology, 579 Qianwangang, Qingdao 266510, P.R. China; Research Center for Hazard Monitoring and Prevention, Wuhan University, 129 Luoyu Road, Wuhan 430079, P.R. China

Y.M. Wang
National Geodetic Survey, Silver Spring, MD 20910, USA

Z.T. Wang
The Institute of Geodesy and Geodynamics, Chinese Academy of Surveying and Mapping, 16 Bei Tai Ping Lu, 100039, Beijing, P.R. China

F. Wild
Geodetic Institute, University of Karlsruhe, Englerstr 7, D-76128 Karlsruhe, Germany, e-mail: wild@gik.uni-karlsruhe.de

A. Xiang
Institute of Seismology, CEA, Wuhan 430071, P.R. China

Y. Xiong
Department of Geomatic Engineering, Southwest Jiaotong University, Chendu 610031, P.R. China

C. Xu
Department of Geomatics Engineering, The University of Calgary, 2500 University Drive N.W., Calgary, Alberta, Canada T2N 1N4, e-mail: xuc@ucalgary.ca

C.Q. Xu
School of Geodesy & Geomatics, Wuhan University, 129 Luoyu Road, Wuhan 430079, P.R. China; Key Laboratory of Geomatics and Digital Technology of Shandong Province, Shandong University of Science and Technology, 579 Qianwangang, Qingdao 266510, P.R. China; Research Center for Hazard Monitoring and Prevention, Wuhan University, 129 Luoyu Road, Wuhan 430079, P.R. China

R. Xu
Center for Geomation Engineering, Southwest Jiaotong University, Chengdu, P.R. China

H. Yin
Earthquake Administration of Shandong Province, Jinan 250014, P.R. China; Department of Geomatic

Engineering, Southwest Jiaotong University, Chengdu 610031, P.R. China

L. Yuan
Center for Geomation Engineering, Southwest Jiaotong University, Chengdu, P.R. China

C. Zhang
Department of Geodesy and Navigation Engineering, Zhengzhou Institute of Surveying and Mapping, Longhai Middle Road, No. 66#, Zhengzhou, Henan Province, P.R. China

H.M. Zhang
School of Power and Mechanical Engineering, Wuhan University, Hubei 430072, P.R. China

Q. Zhang
College of Geological Engineering and Geomatics, Chang'an University, No. 126 Yanta Road, Xi'an, Shaanxi, P.R. China

X. Zhang
School of Geodesy and Geomatics, Wuhan University, 129, Luoyu Road, Wuhan 430079, P.R. China

C. Zhao
College of Geological Engineering and Geomatics, Chang'an University, No. 126 Yanta Road, Xi'an, Shaanxi, P.R. China

D. Zhao
School of Geodesy and Geomatics, Wuhan University, Hubei Province, P.R. China; Department of Geodesy and Navigation Engineering, Zhengzhou Institute of Surveying and Mapping, Longhai Middle Road, No. 66#, Zhengzhou, Henan Province, P.R. China

J.H. Zhao
School of Geodesy and Geomatics, Wuhan University, Wuhan, Hubei 430079, P.R. China

Q.L. Zhao
GNSS Research Center, Wuhan University, Wuhan, Hubei, P.R. China

L. Zhou
Center for Geomation Engineering, Southwest Jiaotong University, Chengdu, P.R. China

X.W. Zhou
Department of Survey Engineering and Geomatics, Central South University, Changsha, Hunan Province 410083, P.R. China, e-mail: zhouxwcsu@hotmail.com

J.J. Zhu
Department of Survey Engineering and Geomatics, Central South University, Changsha, Hunan Province 410083, P.R. China

P. Zhu
Royal Observatory of Belgium, Belgium

X. Zhu
School of Computer Science and Technology, Shandong University of Technology, Zibo, P.R. China

Z.R. Zou
Department of Survey Engineering and Geomatics, Central South University, Changsha, Hunan Province 410083, P.R. China

Part I
Satellite Gravity and Geodynamics

Do We Need New Gravity Field Recovery Techniques for the New Gravity Field Satellites?

K.H. Ilk, A. Löcher, T. Mayer-Gürr
Institute of Theoretical Geodesy, University of Bonn, Nussallee 17, D-53115 Bonn, Germany

Abstract. The classical approach of satellite geodesy consists in deriving the spherical harmonic coefficients representing the gravitational potential from an analysis of accumulated orbit perturbations of artificial satellites with different altitudes and orbit inclinations. This so-called differential orbit improvement technique required the analysis of rather long arcs of days to weeks; it was the adequate technique for satellite arcs poorly covered with observations, mainly precise laser ranging to satellites. The situation changed dramatically with the new generation of dedicated gravity satellites such as CHAMP, GRACE and – in a couple of months – GOCE. These satellites are equipped with very precise sensors to measure the gravity field and the orbits. The sensors provide a very dense coverage with observations independent from Earth based observation stations. The measurement concepts can be characterized by an in-situ measurement principle of the gravitational field of the Earth. In the last years various recovery techniques have been developed which exploit these specific characteristics of the in-situ observation strategy. This paper gives an overview of the various gravity field recovery principles and tries to systemize these new techniques. Alternative in-situ modelling strategies are presented based on the translational and rotational integrals of motion. These alternative techniques are tailored to the in-situ measurement characteristics of the innovative type of satellite missions. They complement the scheme of in-situ gravity field analysis techniques.

Keywords. CHAMP, GRACE, GOCE, differential orbit improvement, in-situ measurement principle, integrals of motion, energy integral, balance equations, gravity field recovery

1 Introduction

The success of the Global Navigation Satellite Systems (GNSS), the development of microcomputer technology and the availability of highly sophisticated sensors enabled space borne concepts of gravity field missions such as CHAMP and GRACE and – to be realized in a couple of months – GOCE. The innovative character of these missions is based on the continuous and precise observations of the orbits of the low flying satellites and the extremely precise range and range-rate K-band measurements between the satellites in case of GRACE. In addition, the surface forces acting on these satellites are measured and can be considered properly during the recovery procedure. In case of GOCE components of the gravity gradient are measured by a gravity gradiometer. The orbit decay of GOCE is compensated by a feedback system coupled with the measurement of the surface forces acting on the satellite so that the kinematically computed orbit is purely gravity field determined.

For the analysis of the observations frequently the classical approach of satellite geodesy has been applied. It consists basically in deriving the spherical harmonic coefficients representing the gravitational potential from an analysis of accumulated orbit perturbations of artificial satellites with different altitudes and orbit inclinations and of sufficient arc lengths. This was an indispensable requirement in case of the satellites available during the last three decades with its poor coverage with observations. On the other hand, the results based on the data from satellite missions such as CHAMP and GRACE demonstrated that a variety of satellites with varying inclinations and altitudes is not necessary for the new generation of dedicated gravity satellites. The measurement concept of these missions can be characterized by an in-situ principle and the analysis of accumulated orbit perturbations caused by the inhomogeneous structure of the gravity field seems to be not necessary. The question arises whether the gravity field recovery techniques which were tailored to the classical observation configurations are still the proper tools for these new observation scenarios?

In the following section we will shortly characterize the classical techniques of satellite geodesy and point out the characteristical features of these techniques. Then a scheme of alternative techniques is sketched, which tries to take into account the characteristical features of the innovative type of satellite missions. Gravity field recovery results have demonstrated that very precise competitive models can be achieved with these new in-situ techniques.

2 The Classical Techniques of Satellite Geodesy

The classical techniques of satellite geodesy are based on the use of satellites as high targets, as test bodies following the force function acting on the satellites and as platforms carrying sensors to detect various features of the Earth system by remote sensing principles.

The determination of the gravitational field and selected position coordinates of terrestrial observation stations by using the satellites as test masses can be performed by a differential orbit determination procedure which is based on the classical (in most cases non-relativistic) Newton–Euler formalism

$$\frac{\mathrm{d}}{\mathrm{d}t}\mathbf{p}(t) = \frac{1}{M}\mathbf{K}(\mathbf{r}, \dot{\mathbf{r}}; t) \rightarrow \ddot{\mathbf{r}} = \mathbf{a}, \tag{1}$$

with the force function $\mathbf{K}(\mathbf{r}, \dot{\mathbf{r}}; t)$ or the specific force function $\mathbf{a}$, the position, velocity and the acceleration vectors $\mathbf{r}$, $\dot{\mathbf{r}}$ and $\ddot{\mathbf{r}}$, as well as the linear momentum $\mathbf{p}$. A numerical as well as an analytical perturbation strategy has been applied, frequently in a complementary way.

The *numerical perturbation concept* can be characterized by the definitive orbit determination process where differential corrections to the various observed or unknown parameters are determined numerically. It is based on the basic geometric relation

$$\mathbf{r}_i(t) = \mathbf{R}_{li}(t) + \mathbf{R}_l(t), \tag{2}$$

with the geocentric position vector $\mathbf{r}_i(t)$ to the satellite i, the respective topocentric position vector $\mathbf{R}_{li}(t)$, referred to the observation station l and the station vector $\mathbf{R}_l(t)$. This equation constitutes the *observation model* which reads for a specific observation time t_k after inserting the observations $\bar{\mathbf{b}}_i$ (ranges, direction elements, etc.) and the approximate values for the (unknown) station coordinates $\mathbf{x}_S^0$ and the respective residuals $\mathrm{d}\mathbf{b}_i$ and corrections to the station coordinates $\mathrm{d}\mathbf{x}_S$

$$\mathbf{r}_i(t_k) = \mathbf{R}_{li}\left(t_k; \bar{\mathbf{b}}_i + \mathrm{d}\mathbf{b}_i\right) + \mathbf{R}_l\left(t_k; \mathbf{x}_S^0 + \mathrm{d}\mathbf{x}_S\right). \tag{3}$$

The *orbit model* is based on Newton–Euler's equation of motion

$$\ddot{\mathbf{r}}_i(t) = \mathbf{a}_F(t; \mathbf{x}_F) + \mathbf{a}_D(t; \mathbf{x}_i), \tag{4}$$

where the specific force function is composed of the Earth-related specific force function $\mathbf{a}_F(t; \mathbf{x}_F)$ with the parameters $\mathbf{x}_F$ and the orbit-related specific disturbance forces $\mathbf{a}_D(t; \mathbf{x}_i)$ with the corresponding model parameters $\mathbf{x}_i$. This equation has to be integrated twice based on the initial values α_i^0 for the orbit i, so that the non-linear model results in

$$\begin{aligned} &\mathbf{r}_i(t_k; \alpha_i^0 + \mathrm{d}\alpha_i, \mathbf{x}_i^0 + \mathrm{d}\mathbf{x}_i, \mathbf{x}_F^0 + \mathrm{d}\mathbf{x}_F) = \\ &= \mathbf{r}_i(t_k, \bar{\mathbf{b}}_i + \mathrm{d}\mathbf{b}_i, \mathbf{x}_S^0 + \mathrm{d}\mathbf{x}_S). \end{aligned} \tag{5}$$

A linearization leads to the so-called mixed adjustment model. The partial differentials are determined numerically by integrating the variational equations or by approximating the partial differentials by partial differences. Obviously, this model requires satellite arcs of sufficient lengths because of two reasons. On the one hand, the coverage of the satellite arcs with observations was very poor in the past compared to the situation nowadays. Therefore, to achieve a sufficient redundancy it was necessary to use medium or long arcs. On the other hand, to cover the characteristic periodic and secular disturbances caused by the small corrections to the approximate force function parameters it was necessary – at least useful – to use medium or long satellite arcs as well.

This fact becomes even more visible by having a closer look at the *analytical perturbation strategy*. The explicit Lagrange's perturbation equations expressed by classical Keplerian elements $a, i, e, \Omega, \omega, \sigma$ and the disturbing potential R read, e.g. for the orbit inclination i and the right ascension of the ascending node Ω

$$\begin{aligned} \frac{\mathrm{d}i}{\mathrm{d}t} &= \frac{1}{na^2\sqrt{1-e^2}\sin i}\left(\cos i\frac{\partial R}{\partial \omega} - \frac{\partial R}{\partial \Omega}\right), \\ \frac{\mathrm{d}\Omega}{\mathrm{d}t} &= \frac{1}{na^2\sqrt{1-e^2}\sin i}\frac{\partial R}{\partial i}. \end{aligned} \tag{6}$$

Inserting Kaula's expansions of the disturbing function in terms of the Keplerian elements leads to the famous Kaula's perturbation equations, with the inclination function F_{nmp}, the excentricity function G_{npq}, etc. (refer to Kaula, 2000, for the explanation of additional quantities):

$$\frac{\mathrm{d}i}{\mathrm{d}t} = \sum_{n,m,p,q} \mathrm{GM}_{\otimes} a_{\otimes}^{n} \frac{F_{nmp} G_{npq} S'_{nmpq}}{\sqrt{\mathrm{GM}_{\otimes} a \left(1-e^2\right)} a^{n+1} \sin i} \cdot \left((n-2p)\cos i - m\right),$$
$$\frac{\mathrm{d}\Omega}{\mathrm{d}t} = \sum_{n,m,p,q} \mathrm{GM}_{\otimes} a_{\otimes}^{n} \frac{\partial F_{nmp}/\partial i \; G_{npq} S_{nmpq}}{\sqrt{\mathrm{GM}_{\otimes} a \left(1-e^2\right)} a^{n+1} \sin i}. \tag{7}$$

These equations demonstrate after a careful analysis that the secular effects and the various periodicities can be detected only with arcs of sufficient length which are able to cover these typical disturbance patterns of the Keplerian elements. As typical effects we only want to mention the dependency of the rotation of the nodal line of the orbit plane and the line of apsides by the zonal spherical harmonics. The situation is similar also in case of the numerical perturbation techniques. The practical experiences underline these numerical characteristics of the perturbation strategies.

3 What Is New with the New Gravity Field Satellite Missions?

A common feature of the new gravity field measurement techniques is the fact that the differences of the free-fall motion of test masses is used to derive more or less in-situ the field strength of the gravity field. This is obvious in case of Satellite Gravity Gradiometry (SGG); here the relative acceleration of two test masses M_1 and M_2 in the sensitivity axis $\mathbf{r}_{12}$ is measured. The main part of the acceleration is represented by the tidal force field $\mathbf{G}_{(21)\otimes}$ of the Earth which can be approximated by the gravitational tensor $\nabla \mathbf{g}_{\otimes}$:

$$\ddot{\mathbf{r}}_{12} = \mathbf{r}_{12} \cdot \nabla \mathbf{g}_{\otimes}. \tag{8}$$

There is no basic difference to the measurement principle in case of Satellite-to-Satellite Tracking (SST) in the low–low mode where the Earth's gravity field is measured also in form of the tidal field acting on the relative motion of two satellites. It reads with the line-of-sight unit vector $\mathbf{e}_{12}$, the reduced mass μ_{12} and the mutual gravitational attraction of both satellites $\mathbf{K}_{21}$:

$$\mathbf{e}_{12} \cdot \ddot{\mathbf{r}}_{12} = \frac{1}{\mu_{12}} \left(\mathbf{K}_{21} + \mathbf{G}_{(21)\otimes}\right) \cdot \mathbf{e}_{12}. \tag{9}$$

In this case the tidal force $\mathbf{G}_{(21)\otimes}$ cannot be approximated with sufficient accuracy by the gravitational tensor. The same principle holds also in case of the free-fall absolute gravimetry or by the use of precisely determined kinematical orbits for gravity field recovery; here the free fall of a test mass with respect to the gravity field of the Earth is observed. The only difference to low-low-SST is the fact that the specific force function is dominated mainly by the gravitational acceleration of the Earth, $\mathbf{g}_{\otimes}$, and not by the tidal force field $\mathbf{G}_{(21)\otimes}$ as in case of low-low-SST or SGG:

$$\ddot{\mathbf{r}} = \mathbf{g}_{\otimes}. \tag{10}$$

Obviously, the in-situ character of these measurement principles does not require the analysis of long arcs with respect to accumulated gravity field effects, because the gravity field is detected more or less directly. It should be pointed out that in all these different measurement scenarios the in-situ observations contain the complete spectral band of the gravity field. Therefore, the frequently expressed argument that long wavelength features of the gravity field cannot be detected in such an in-situ way is certainly not true. The restrictions with respect to the signal content in certain observables are caused by the spectral limitations of the measurement apparatus, such as in case of a satellite gravity gradiometer, as envisaged for the GOCE mission.

4 A Systematic of In-Situ Gravity Field Recovery Techniques

We define in-situ gravity field recovery concepts as those which are based in principle on the precisely observed free-fall motion of a test mass within the Earth's gravity field. This group of gravity measurement techniques covers not only the absolute gravity measurement concepts based on the free-fall principle, but also SGG and SST in the high–low or low–low mode or by analyzing short precisely determined kinematic arcs (POD) with respect to the Earth (Figure 1). In the following, we will refer without loss of generality on the motion of a single satellite or test mass with respect to the Earth, but formulated in an Inertial Reference System.

The gravity field recovery techniques can be divided in three analysis levels (Figure 2). The *analysis level 1* is based directly on the observed precisely determined kinematic positions, derived from GNSS observations. It is related directly to the specific force function via an integral equation of Fredholm type (with the integral kernel $K\left(t, t'\right)$):

$$\mathbf{r}(t) = \bar{\mathbf{r}}(t) - \int_{t_0}^{t} K\left(t, t'\right) \mathbf{g}(\mathbf{r}; t') \mathrm{d}t'. \tag{11}$$

This equation has been applied by Mayer-Gürr et al. (2005) for the determination of the precise

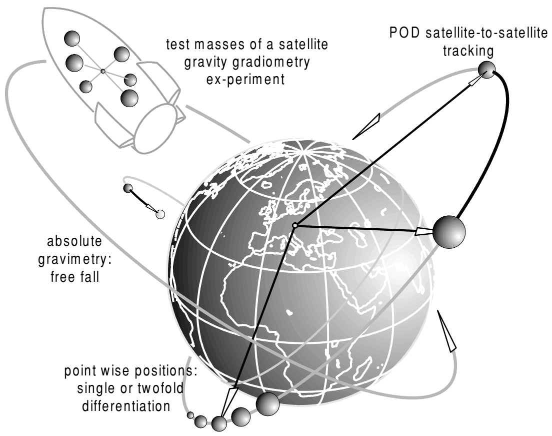

Fig. 1. In-situ free fall gravity field measurement techniques.

CHAMP gravity field models CHAMP-ITG 01E, 01K and 01S. The solution of this equation can be formulated as well in the spectral domain:

$$\mathbf{r}(t) = \bar{\mathbf{r}}(t) + \sum_{\nu=1}^{\infty} \mathbf{r}_\nu \sin(\nu\pi\tau), \tag{12}$$

with the normalized time $\tau(t)$. The sinus coefficients are related to the specific force function by the relation (see, e.g., Ilk et al., 2003)

$$\mathbf{r}_\nu = -\frac{2T^2}{\pi^2\nu^2} \int\limits_{\tau'=0}^{1} \sin(\nu\pi\tau')\mathbf{g}(\mathbf{r};\tau')\mathrm{d}\tau'. \tag{13}$$

The *analysis level 2* requires the numerical differentiation of the time series of precise kinematically determined positions at the (left) observation model side and an integration of the force function at the (right) orbit model side. Up to now this possibility has been applied frequently in the last years by various authors to determine the gravity field with a sort of generalized Jacobi or energy integral (see e.g. Jekeli (1999) or Gerlach et al. (2003) for the derivation of the CHAMP gravity field model TUM-1s). The use of energy balance relations for the validation of gravity field models and orbit determination results has been treated by Ilk and Löcher (2003) and Löcher and Ilk (2005). In Löcher and Ilk (2006) new balance equations have been formulated for validation and gravity field recovery.

These various integrals of motion can be derived from Newton's equation of motion starting with an operation which transforms the acceleration term into a function f and the force into a function h. If f has the primitive F, the transformed equation

$$f\left(M, \mathbf{R}, \dot{\mathbf{R}}, \ddot{\mathbf{R}}\right) - h\left(M, \mathbf{R}, \dot{\mathbf{R}}, \mathbf{K}\right) = 0 \tag{14}$$

results by integration over the time interval $[t_0, t]$ in

$$F\left(M, \mathbf{R}, \dot{\mathbf{R}}\right) - \int\limits_{t_0}^{t} h\left(M, \mathbf{R}, \dot{\mathbf{R}}, \mathbf{K}\right)\mathrm{d}t = C. \tag{15}$$

The first term represents the "kinetic" term of the observation model, the second term the force function integral of the orbit model. Figure 3 gives an overview of all possible integrals of translational motion and its functional dependencies and Figure 4 shows a similar flow chart for the integrals of rotational motion (Löcher, 2006).

Despite their dependencies the various balance equations show specific characteristics if they are applied for validation and gravity field determination tasks. Investigations demonstrated that these alternative balance equations show partly much better properties for validation and gravity field improvements than the frequently used Jacobi integral.

The *analysis level 3* requires a twofold numerical differentiation at the observation model side and the direct use of the orbit model. This approach is based directly on Newton's equation of motion, which balances the acceleration vector and the gradient of the gravitational potential. By a twofold numerical differentiation of a moving interpolation polynomial in powers of the (normed) time τ, with a proper degree N,

$$\mathbf{r}(\tau) = \sum_{n=0}^{N} \tau^n \sum_{j=0}^{N} w_{nj}\mathbf{r}(t_k + \tau_j), \tag{16}$$

the parameters of the orbit model can be determined directly based on the discretized Newton–Euler

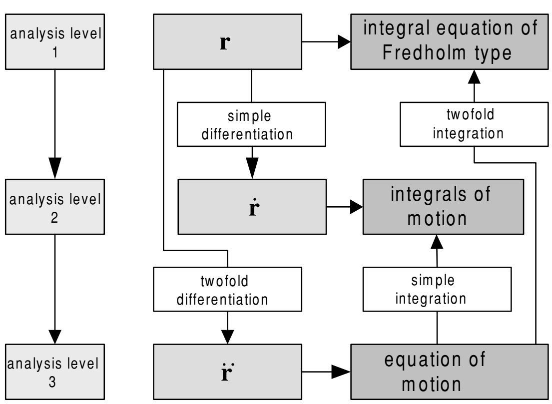

Fig. 2. The three analysis levels of the in-situ gravity field recovery techniques.

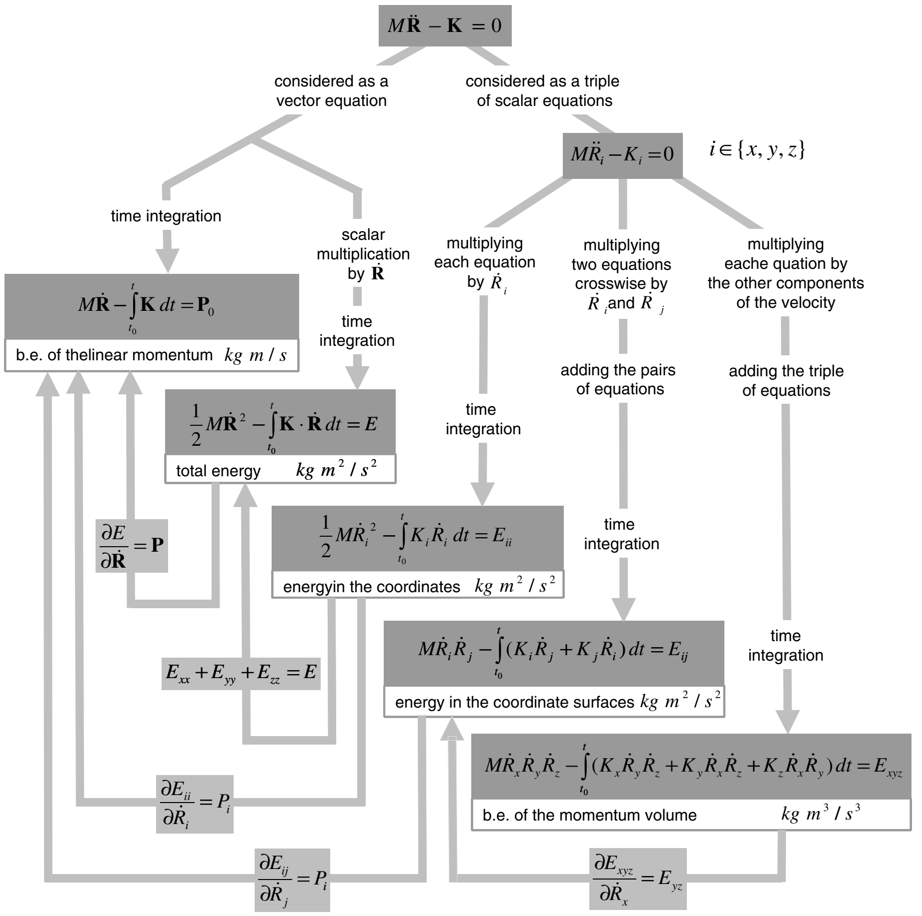

Fig. 3. Integrals of translational motion and its functional dependencies.

equation of motion. This technique has been successfully applied for the gravity field recovery based on kinematical orbits of CHAMP (Reubelt et al., 2003). A similar technique based on weighted averages of three successive positions in the form of

$$\ddot{\mathbf{r}}(t) = \frac{1}{M}\mathbf{K}(\mathbf{r}, \dot{\mathbf{r}};\, t) = \frac{\mathbf{r}(t-\Delta t) - 2\mathbf{r}(t) + \mathbf{r}(t-\Delta t)}{(\Delta t)^2} \tag{17}$$

has been applied successfully by Ditmar et al. (2006). Obviously the latter analysis level requires in principle only a subsequent set of precise positions which represents again a short arc and the procedure can again be characterized by the in-situ measurement principle as defined before.

5 Conclusions

In this paper alternative in-situ gravity field recovery procedures, applied in the last couple of years, have been reviewed and additional ones have been proposed. These recent techniques are tailored to the specific characteristics of the new gravity field missions. In the past, only few observations, mostly laser ranging data to the satellites were available. This fact required the use of long arcs and the analysis of accumulated gravity field effects in the observations to cover the periodicities of specific gravity field disturbances. Numerical or analytical differential orbit improvement techniques have been applied to solve for the unknown parameters. Especially the analytical techniques required the modelling of the gravity field by series of spherical harmonics. A disadvantage of these techniques is the accumulation of improperly modelled disturbing forces. The requirement of comparably long arcs causes problems also in case of gaps in the series of observations.

The recent gravity field missions such as CHAMP, GRACE and – in a couple of months – GOCE are characterized by the fact that the orbits show a very dense coverage of precise GNSS observations

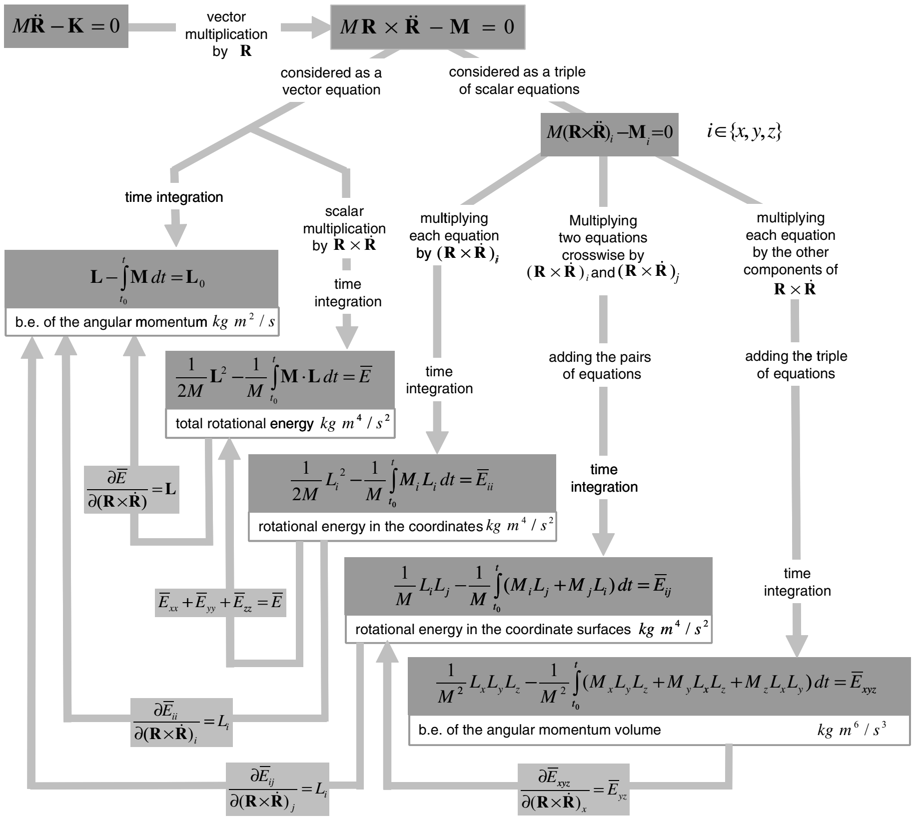

Fig. 4. Integrals of rotational motion and its functional dependencies.

and – as a result – very precise kinematical orbits. In addition, highly precise range and range-rate measurements between the GRACE satellites are available and very precise gravity gradient components in case of GOCE will be available soon. Instead of analyzing accumulated orbit disturbances, the gravity field can be determined in a more direct way by in-situ measurement and analysis techniques by using short arcs. This has some advantages: the accumulation of improperly modelled disturbing forces can be avoided. Observation gaps are not critical and it is possible to perform regional gravity field refinements by space localizing base functions. Various investigations have shown that there are additional gravity field signals in the observations over rough gravity field regions.

In a forthcoming paper under preparation gravity field recovery tests will be performed based on these different in-situ analysis techniques.

Acknowledgement

The support of BMBF (Bundesministerium für Bildung und Forschung) and DFG (Deutsche Forschungs Gemeinschaft) of the GEOTECHNOLOGIEN programme is gratefully acknowledged.

References

Ditmar P, Kuznetsov V, van Eck van der Sluijs AA, Schrama E, Klees R (2006) "DEOS_CHAMP-01C_70": a model of the Earth's gravity field computed from accelerations of the CHAMP satellite, Journal of Geodesy (2006) 79: 586–601.

Gerlach C, Földvary L, Švehla D, Gruber T, Wermuth M, Sneeuw N, Frommknecht B, Oberndorfer H, Peters T, Rothacher M, Rummel R, Steigenberger P (2003) A CHAMP-only gravity field model from kinematic orbits using the energy integral, Geophysical Research Letters (2003) 30(20), 2037.

Ilk KH, Feuchtinger M, Mayer-Gürr T (2003) Gravity Field Recovery and Validation by Analysis of Short Arcs of a Satellite-to-Satellite Tracking Experiment as CHAMP and GRACE, In: F. Sansò (ed.) A Window on the Future of Geodesy, IUGG General Assembly 2003, Sapporo, Japan, International Association of Geodesy Symposia, Vol. 128, pp. 189–194, Springer.

Ilk KH, Löcher A (2003) The Use of Energy Balance Relations for Validation of Gravity Field Models and Orbit Determination Results, In: F. Sansò (ed.) A Window on the Future of Geodesy, IUGG General Assembly 2003, Sapporo, Japan, International Association of Geodesy Symposia, Vol. 128, pp. 494–499, Springer.

Jekeli Ch (1999) The determination of gravitational potential differences from satellite-to-satellite tracking, Celestial

Mechanics and Dynamical Astronomy (1999) 7582, pp. 85–100.
Kaula WM (2000) Theory of Satellite Geodesy, Applications of Satellites to Geodesy, Dover Publications, INC, Mineola, New York.
Löcher A (2006) A scheme of integrals of motion for gravity field determination based on precisely observed low Earth satellites, poster presented at the General Assembly 2006 of the EGU, April 02–07, 2006, Vienna, Austria.
Löcher A, Ilk KH (2005) Energy Balance Relations for Validation of Gravity Field Models and Orbit Determinations Applied to the Results of the CHAMP Mission, In: C. Reigber, H. Lühr, P. Schwintzer, J. Wickert (Eds.) Earth Observation with CHAMP, Results from Three Years in Orbit, pp. 53–58, Springer.
Löcher A, Ilk KH (2006) A Validation Procedure for Satellite Orbits and Force Function Models Based on a New Balance Equation Approach, In: Proceedings of the Internat. Symposium Dynamic Planet 2005, Monitoring and Understanding a Dynamic Planet with Geodetic and Oceanographic Tools, August 22–26, 2005, Cairns, Australia.
Mayer-Gürr T, Ilk KH, Eicker A, Feuchtinger M (2005) ITG-CHAMP01: a CHAMP gravity field model from short kinematical arcs of a one-year observation period, Journal of Geodesy (2005) 78:462–480.
Reubelt T, Austen G, Grafarend EW (2003) Harmonic analysis of the Earth's gravitational field by means of semi-continuous ephemerides of a low Earth orbiting GPS-tracked satellite. Case study: CHAMP, Journal of Geodesy (2003) 77:257–278.

A Localizing Basis Functions Representation for Low–Low Mode SST and Gravity Gradients Observations

W. Keller
Institute of Geodesy, Universität Stuttgart, Geschwister-Scholl-Str. 24D, D-70174 Stuttgart, Germany

Abstract. For geophysical/ oceanographic/ hydrological applications of dedicated gravity field missions regional gravity field solutions are of higher interest than the usual global solutions. In order to derive regional solutions, so-called in-situ observations like line-of-sight accelerations or satellite gradiometry data are optimal, since they do not change, if the potential outside a infinitesimal neighborhood of the observation point changes. Therefore, in-situ observations do not introduce influences from outside the region under consideration. The localization on the observation-side has to be balaced by a localization on the model-side.

The usual spherical harmonics representation is not appropriate for the desired regional solution, because spherical harmonics have a global support. In order to model local phenomena by base functions with a global support, the superposition of a large number of those global base functions is necessary.

For this reason the paper aims at an establishment of a direct relationship between several types of in-situ observations and the unknown coefficients of a localizing basis functions representation of the regional gravity field.

Keywords. Satellite-to-satellite tracking, localizing base functions, representation of rotation group, Wigner functions

1 Introduction

The temporal data-sampling of the Earth's gravity field by an orbiting satellite is transformed via the orbital movement of the satellite and the rotation of the Earth into a spatial sampling on the surface of a sphere. In general the resulting data-spacing on the Earth is non-uniform and coarser than the theoretical resolution limit, stemming from the temporal data sampling. The usual technique for the analysis of dedicated gravity field satellite missions is the the representation of the resulting gravity field solution as a series expansion in spherical harmonics. Due to the fact that the related surface spherical harmonics have a global support on the unit sphere and the data sampling is non-uniform, the theoretical resolution limit, deduced from the temporal data sampling rate, cannot be reached and the spherical harmonics solution includes a certain smoothing of details in the gravity field. This becomes obvious when the original observations are compared with synthetic observation, computed from an existing gravity field solution. In Figure 1 the difference between the original GRACE range-rates and the synthetic range-rates computed from the GRACE gravity field solution GGSM02 is plotted. It is clearly visible that the difference is not white noise but contains a residual signal. This residual signal is caused by the fact that, due to their global support and due to the given data-distribution, spherical harmonics are not able to capture all signal details. In order to capture also the residual signal components, two measures have to be taken

1. Representation of the residual (so far not captured gravity field) by localizing basis functions in the region under consideration.
2. Usage of so-called in-situ observation, as e.g. line-of-sight accelerations or satellite gradiometry data, for sensing of the residual field, to make sure that no influences from outside the region under consideration enter the observations.

In Keller and Sharifi (2005) it was shown that with proper reductions low–low mode SST observations can be treated as along-track gravity gradients. Therefore, the results to be presented here for gravity gradients do implicitly also hold for low–low mode SST observations.

So far the only in-situ observation with a clear relationship to the unknown parameters of a localizing basis function representation are the radial gravity tensor components observations (cf. Freeden et al. (1999)). To the author's knowledge no

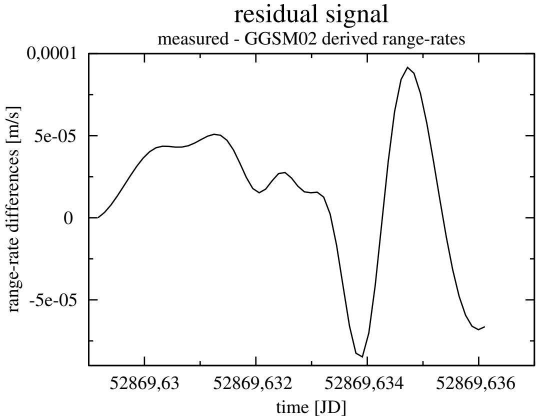

Fig. 1. Difference between original range-rates and synthetic range-rates of GRACE along a 10 min arc.

other gravity-field related observations have been expressed in a simple analytic form as functionals on localizing base functions in geodetic literature so far. The paper aims at an establishment of simple relationships also for the along-track and the out-of-plane gravity tensor components.

2 State-of-the-Art

Gravity field modeling by localizing base functions means to approximate the unknown potential V by a linear combination of special base functions:

$$V(\mathbf{x}) = \sum_i c_i \psi_i(\mathbf{x}). \tag{1}$$

Here the base functions ψ_i are localizing base functions having the following structure

$$\psi_i(\mathbf{x}) := \psi(g_i^{-1}\mathbf{x}), \quad g_i \in SO(3) \tag{2}$$

and

$$\psi(\mathbf{x}) = \sum_{n\in\mathbb{N}} \sigma_n^2 P_n(\mathbf{e}_3 \cdot \frac{\mathbf{x}}{\|\mathbf{x}\|}) \tag{3}$$

where P_n are the Legendre-polynomials and $\mathbf{e}_3$ is a unit-vector pointing in the direction of 3rd axis of the underlying cartesian coordinate system. The sequence $\{\sigma_n\}$ controls the decay of the base function ψ. The generic base function ψ is located at the north-pole of the sphere and the actual base functions are the rotated copies of this generic function.

So far the only well-established method to relate in-situ observations to a localizing base function representation of the field is an approach which could be called *spectral modeling*.

Spectral Modeling

Spectral modeling can be applied in those cases, where the gravity field-related observation can be represented by a so called *invariant pseudo-differential operator* (PDO) p on $C^\infty(\sigma_r)$, the space of all infinite often differentiable functions on a sphere of radius r. A PDO is called invariant, if it is invariant against rotations g out of $SO(3)$

$$[pu](g^{-1}\mathbf{x}) = p[u(g^{-1}\mathbf{x})].$$

This leads to the consequence, that all surface spherical harmonics $Y_{n,m}$ of the same degree n are eigenfunctions belonging to the same eigenvalue $p \wedge (n)$

$$pY_{n,m}(\frac{\omega}{r}) = p \wedge (n) \cdot Y_{n,m}(\frac{\omega}{r}). \tag{4}$$

The eigenvalues $p \wedge (n)$ are called the *spherical symbols* of the PDO p.

Examples for invariant PDOs are the radial derivatives and the Poisson operator P_R^r for harmonic upward continuation:

p	$p \wedge (n)$
P_R^r	$\left(\frac{R}{r}\right)^{n+1}$
$\partial u/\partial r$	$-\frac{n+1}{r}$
$\partial^2 u/\partial r^2$	$\frac{(n+1)(n+2)}{r^2}$

From the *addition theorem*

$$\frac{2n+1}{2} P_n(\zeta \cdot \eta) = \sum_{m=-n}^{n} Y_{n,m}(\zeta) Y_{n,m}^*(\eta), \quad \zeta, \eta \in \sigma_1 \tag{5}$$

for each invariant PDO p immediately follows

$$p\psi_i(\mathbf{x}) = \psi_i^p(\mathbf{x}) \tag{6}$$

$$\psi^p(\mathbf{x}) := \sum_{n\in\mathbb{N}} \left(\sigma_n^2 \cdot p \wedge (n)\right) P_n(\mathbf{e}_3 \cdot \frac{\mathbf{x}}{\|\mathbf{x}\|}) \tag{7}$$

Hence the application of an invariant PDO on a base function results in a change of its decay. The spectral modeling assumes that a certain quantity $\Gamma \in C^\infty(\sigma_r)$ is given on the sphere σ_r , which is the image of a unknown function $u \in C^\infty(\sigma_R)$ under the invariant PDO p

$$\Gamma = pu. \tag{8}$$

Both the given data Γ and the unknown function u can be represented as linear combinations of systems of localizing base functions ψ_i^p and ψ_i, respectively.

$$\Gamma = \sum_i c_i \psi_i^p, \quad u = \sum_i d_i \psi_i, \tag{9}$$

with the known coefficients d_i and the unknown coefficients c_i. Which leads via

$$\begin{aligned} \sum_i c_i \psi_1^p = \Gamma = pu \\ = \sum_i d_i p \psi_i \\ = \sum_i d_i \psi_i^p. \end{aligned} \tag{10}$$

to a comparison of coefficients $d_i = c_i$ and from there to the desired solution u. The spectral combination is an inversion-free and stable method, but restricted to first and second order radial derivatives as observations. There is an extended literature about spectral modeling. Without attempting to be close to completeness the following newer references are to be mentioned: Freeden et al. (1999), Freeden and Hesse (2002), Freeden and Maier (2003), and Schmidt et al. (2005, 2006). Unfortunately, the spectral modeling is not directly applicable for along-track and out-of-plane gravity gradients. The idea to relate those observations to a localizing base function representation of the unknown potential is similar to the classical Lagrangian disturbing theory. There the observed orbital disturbances are expressed as linear combination of multi-periodic functions, weighted by the unknown coefficients of the spherical harmonics expansion of the potential. There are two differences between the classical Lagrangian disturbing theory and the development the paper is aiming at:

1. Instead of spherical harmonics here localizing base functions are to be used.
2. Instead of orbital disturbances gravity gradients in three orthogonal directions are used as observations.

The way this goal is to be achieved is similar to the classical Lagrangian disturbing theory: Transformation of the potential representation to a coordinate system, which follows the movement of the satellite cf. Sneeuw (1992).

3 Representation Theory of $SO(3)$

Both the definition of a system of localizing radial basis functions and the establishment of a relationship between such a representation and in-situ observations make use of the representation theory of $SO(3)$. For this purpose the necessary results from representation theory are to be compiled here.

The group of rotations of $\mathbb{R}^3$ around the origin is denoted by $SO(3)$. It consists of real 3-by-3 orthogonal matrices of determinant $+1$. To each $g = u(\gamma)a(\beta)u(\alpha) \in SO(3)$ an operator $\Lambda(g)$ acting on $L^2(\sigma)$ can be associated

$$(\Lambda(g)f)(\omega) := f(g^{-1}\omega), \tag{11}$$

with the matrices a, u given by

$$a(\alpha) := \begin{bmatrix} \cos\alpha & 0 & -\sin\alpha \\ 0 & 1 & 0 \\ \sin\alpha & 0 & \cos\alpha \end{bmatrix} \tag{12}$$

and

$$u(\beta) := \begin{bmatrix} \cos\beta & \sin\beta & 0 \\ -\sin\beta & \cos\beta & 0 \\ 0 & 0 & 1 \end{bmatrix}. \tag{13}$$

Every rotated version $\Lambda(g)\bar{Y}_{nm}$ of a surface spherical harmonic is the following linear combination of the non-rotated surface spherical harmonics of the same degree:

$$\Lambda(g)\bar{Y}_{nm}(\vartheta, \lambda) = \sum_{k=-n}^{n} D(g)_{km}^n \bar{Y}_{nk}(\bar{\vartheta}, \bar{\lambda}), \tag{14}$$

with

$$D_{km}^l(g) = e^{\imath k\alpha} d_{km}^l(\beta) e^{\imath m\gamma}, \tag{15}$$

where $\bar{\vartheta}, \vartheta$ and $\bar{\lambda}, \lambda$ are co-latitude and longitude in the non-rotated and the rotated system, respectively.

The functions $d_{km}^l(\beta)$ are called Wigner-d functions and are defined as follows

$$\begin{aligned} d_{km}^l(\beta) = (-1)^{m-k} \sqrt{\frac{(l+m)!(l-m)!}{(l+k)!(l-k)!}} \\ \times (\sin\frac{\beta}{2})^{m-k} (\cos\frac{\beta}{2})^{k+m} \\ \times P_{l-m}^{(m-k,m+k)}(\cos\beta), \end{aligned} \tag{16}$$

with $P_l^{(m,n)}$ being the Jacobi Polynomials (Vilenkin 1968).

4 Transformation to Orbital System

Local gravity field representation means an approximation of the residual field by rotated versions of the radial base functions

$$\delta V(\omega) = \sum_{i=1}^{N} c_i \psi_i(\omega). \qquad (17)$$

In order to determine the unknown coefficients c_i and the unknown placements $g_1^{-1}\mathbf{e}_3$ in the radial base function representation of the residual field, the residual field has to be related to residual SST or gradiometry observations.

If a body-fixed coordinate system x, y, z is attached to the satellite in such a way that x points in radial, y points in along track and z points in out-of-plane direction (see Figure 2), only for the radial tensor component δV_{xx} a simple relationship

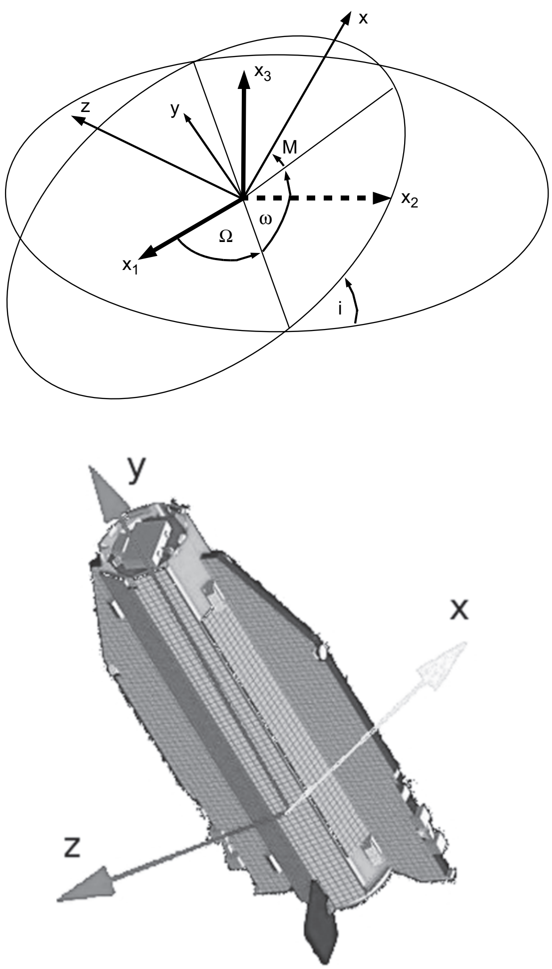

Fig. 2. Body-fixed coordinate system (bottom) and its relationship to the space-fixed system (top).

to the free parameters c_i of the field representation is known. In what follows $SO(3)$ representation theory will be used to establish a similar relationship for the remaining two tensor components $\delta V_{yy}, \delta V_{zz}$. The relationship between the body-fixed and the space fixed system is approximatively given by the following rotation

$$g = u(\Omega - \Theta - \frac{\pi}{2})a(i)u(\frac{\pi}{2} + \omega + M) \qquad (18)$$

where ω, Ω, i, M are the mean elements of the orbital arc under consideration.

The representation of a radial base function in the rotating system is given by

$$\begin{aligned}(\Lambda(g)\psi_i)(\mathbf{x}) &= \Lambda(g) \sum_{n\in\mathbb{N}} \sigma_n \frac{2}{2n+1}\left(\frac{R}{\|\mathbf{x}\|}\right)^{n+1} \sum_{m=-n}^{n} Y_{n,m}(g_i\mathbf{e}_3)Y^*_{n,m}(\frac{\mathbf{x}}{\|\mathbf{x}\|})\\ &= \sum_{n\in\mathbb{N}} \sigma_n \frac{2}{2n+1}\left(\frac{R}{\|\mathbf{x}\|}\right)^{n+1} \sum_{m=-n}^{n} Y_{n,m}(g_i\mathbf{e}_3)\cdot\Lambda(g)Y^*_{n,m}(\frac{\mathbf{x}}{\|\mathbf{x}\|})\\ &= \sum_{n\in\mathbb{N}} \sigma_n \frac{2}{2n+1}\left(\frac{R}{\|\mathbf{x}\|}\right)^{n+1} \sum_{m=-n}^{n} Y_{n,m}(g_i\mathbf{e}_3)\cdot Y^*_{n,m}(g^{-1}\bar{\omega}).\end{aligned}$$

Here, $\bar{\omega}$ is the position of the satellite in the rotating system.

Since for an exact circular orbit $\bar{\omega} = \mathbf{e}_1$ holds also for weakly eccentric orbits approximatively holds:

$$\begin{aligned}(\Lambda(g)\psi_i)(\mathbf{x}) &= \sum_{n\in\mathbb{N}} \sigma_n \frac{2}{2n+1}\left(\frac{R}{\|\mathbf{x}\|}\right)^{n+1} \sum_{m=-n}^{n} Y_{n,m}(g_i\mathbf{e}_3)\cdot Y^*_{n,m}(g^{-1}\mathbf{e}_1)\\ &= \sum_{n\in\mathbb{N}} \sigma_n \left(\frac{R}{\|\mathbf{x}\|}\right)^{n+1} P_n((g_i\mathbf{e}_3\cdot(g^{-1}\mathbf{e}_1)).\end{aligned}$$

Besides this an equivalent representation of $(\Lambda(g)\psi_i)(\mathbf{x})$ is useful:

$$(\Lambda(g)\psi_i)(\mathbf{x}) = \sum_{n\in\mathbb{N}} \sigma_n \frac{2}{2n+1}\left(\frac{R}{\|\mathbf{x}\|}\right)^{n+1}$$

$$\sum_{m=-n}^{n} Y_{n,m}(g_i\mathbf{e}_3)\cdot\Lambda(g)Y^*_{n,m}(\frac{\mathbf{x}}{\|\mathbf{x}\|})$$
$$=\sum_{n\in\mathbb{N}}\sigma_n\frac{2}{2n+1}\left(\frac{R}{\|\mathbf{x}\|}\right)^{n+1}$$
$$\sum_{m=-n}^{n} Y_{n,m}(g_i\mathbf{e}_3)\cdot\Lambda(g)Y^*_{n,m}(\frac{\mathbf{x}}{\|\mathbf{x}\|})$$
$$=\sum_{n\in\mathbb{N}}\sigma_n\frac{2}{2n+1}\left(\frac{R}{\|\mathbf{x}\|}\right)^{n+1}$$
$$\sum_{m=-n}^{n} Y_{n,m}(g_i\mathbf{e}_3)e^{\imath m(\frac{\pi}{2}+\omega+M)}\,.$$
$$\sum_{k=-n}^{n} e^{\imath k(\Omega-\Theta-\frac{\pi}{2})}d^n_{m,k}(i)Y_{n,k}(\bar{\omega}).$$

With the introduction of the abbreviations

$$F_{n,m}(i,\Omega,\Theta):=\sum_{k=-n}^{n} e^{\imath[k(\Omega-\Theta-\frac{\pi}{2})]}d^n_{k,m}(i)Y_{n,k}(\bar{\omega}) \tag{19}$$

and

$$G_{n,m}(g_i,\omega,M):=Y_{n,m}(g_i\mathbf{e}_3)e^{\imath m(\frac{\pi}{2}+\omega+M)} \tag{20}$$

this leads to the final result

$$(\Lambda(g)\psi_i)(\mathbf{x})=\sum_{n\in\mathbb{N}}\sigma_n\frac{2}{2n+1}\left(\frac{R}{\|\mathbf{x}\|}\right)^{n+1} \sum_{m=-n}^{n} G_{n,m}(g_i,\omega,M)\times \times F_{n,m}(i,\Omega,\Theta) \tag{21}$$

5 Observation Equations

The second order derivatives in

- x -radial direction
- y -along-track direction
- z -across-track direction

are given by (see Koop 1993):

$$\frac{\partial^2\Lambda(g)\psi_i}{\partial x^2}=\frac{\partial^2\Lambda(g)\delta V(\omega)}{\partial r^2}$$
$$=\sum_{n\in\mathbb{N}}\sigma_n\left(\frac{R}{\|\mathbf{x}\|}\right)^{n+3}\times\frac{(n+1)(n+2)}{R^2}\times P_n(g_i\mathbf{e}_3\cdot(g^{-1}\mathbf{e}_1))$$

$$\frac{\partial^2\Lambda(g)\psi_i}{\partial y^2}=\frac{1}{a^2}\frac{\partial^2\Lambda(g)\delta V(\omega)}{\partial(M+\omega)^2}+\frac{1}{a}\frac{\partial\Lambda(g)\delta V(\omega)}{\partial r} \tag{22}$$
$$=\sum_{n\in\mathbb{N}}\sigma_n\frac{(n+1)}{Ra}\left(\frac{R}{\|\mathbf{x}\|}\right)^{n+2}\times P_n(g_i\mathbf{e}_3)$$
$$-\sum_{n\in\mathbb{N}}\sigma_n\frac{2}{(2n+1)a^2}\left(\frac{R}{\|\mathbf{x}\|}\right)^{n+1}\sum_{m=-n}^{n} m^2Y_{n,m}(g_i\mathbf{e}_3)Y_{n,m}(g\mathbf{e}_1)$$

$$\frac{\partial^2\Lambda(g)\psi_i}{\partial z^2}=\frac{\partial^2\Lambda(g)\delta V(\omega)}{a^2\sin^2(M+\omega)\partial i^2}+\frac{1}{a}\frac{\partial\Lambda(g)\delta V(\omega)}{\partial r}$$
$$=\sum_{n\in\mathbb{N}}\sigma_n\frac{(n+1)}{Ra}\left(\frac{R}{\|\mathbf{x}\|}\right)^{n+2}\times P_n(g_i\mathbf{e}_3)$$
$$+\frac{1}{a^2\sin^2(M+\omega)}\sum_{n\in\mathbb{N}}\sigma_n\frac{2}{2n+1}\left(\frac{R}{\|\mathbf{x}\|}\right)^{n+1}\sum_{m=-n}^{n}\times G_{n,m}(g_i,\omega,M)\cdot\frac{\partial^2F_{n,m}(i,\Omega,\Theta)}{\partial i^2}$$

Relations (22) establish the analytic relationships between the localizing base functions representation and gravity gradient observations in three orthogonal directions.

6 Numerical Example

In order to verify the derivations above, a simple forward computation was carried out. For a single GOCE arc the along track gravity-gradient tensor component δV_{yy} was computed twice: Once by numerical orbit computation and once using the relations (22). As gravity field a three-basis functions regional model δV on top of GGSM02 was used.

In order to relate the arc to the residual potential, a projection of the satellite ground track onto the residual potential is displayed in Figure 3. Along this track the quantities δV_{yy} were computed both numerically and analytically. In Figure 4 the difference between the true gradiometry signal (i.e. the